Impact of photo- and thermooxidative ageing of NBR/PVC blends on the formation of cracks

Clara Thoral, Gérald Soulagnet, Pierre-Olivier Bussiere, Sandrine Therias

▶ **To cite this version:**

Clara Thoral, Gérald Soulagnet, Pierre-Olivier Bussiere, Sandrine Therias. Impact of photo- and thermooxidative ageing of NBR/PVC blends on the formation of cracks. Polymer Degradation and Stability, 2024, 220, pp.110633. 10.1016/j.polymdegradstab.2023.110633 . hal-04441910

HAL Id: hal-04441910
https://uca.hal.science/hal-04441910v1

Submitted on 16 Oct 2024

HAL is a multi-disciplinary open access archive for the deposit and dissemination of scientific research documents, whether they are published or not. The documents may come from teaching and research institutions in France or abroad, or from public or private research centers.

L'archive ouverte pluridisciplinaire **HAL**, est destinée au dépôt et à la diffusion de documents scientifiques de niveau recherche, publiés ou non, émanant des établissements d'enseignement et de recherche français ou étrangers, des laboratoires publics ou privés.

Distributed under a Creative Commons Attribution - NonCommercial - NoDerivatives 4.0 International License

Impact of photo- and thermooxidative ageing of NBR/PVC blends on the formation of cracks

Clara Thoral[1,2], Gérald Soulagnet[2], Pierre-Olivier Bussiere[1], Sandrine Therias[1*]

[1]*Université Clermont Auvergne, CNRS, Clermont Auvergne INP, ICCF, F-63000, Clermont-Ferrand, France*

[2]*Trelleborg Industrie SAS, ZI La Combaude, Rue de Chantemerle, F-63050 Clermont-Ferrand, France*

Abstract

Photo- and thermal ageing of nitrile butadiene rubber (NBR)/poly(vinyl chloride) (PVC) blends cured with sulfur and a vulcanization agent have been studied. Characterization of the aged NBR/PVC films was performed by using FTIR and UV–visible spectroscopy, DMTA, Shore A hardness and swelling measurements. The objective was to understand the formation of cracks upon ageing and to put in evidence correlations between the different scales: from chemical structure to functional properties.

Keywords: Nitrile butadiene rubber (NBR), poly(vinyl chloride) (PVC), photooxidation, thermooxidation, cracks, multiscale correlations

1. Introduction

Nitrile butadiene rubber (NBR) or nitrile rubber is a copolymer formed by butadiene and acrylonitrile monomers, providing flexibility at low temperature and oil resistance. The majority of nitrile rubbers have an acrylonitrile content between 19% and 40%; the higher the content is, the higher the resistance to hydrocarbons will be, but it will impact properties at low temperatures. These particular characteristics make it a material of interest for the automotive sector, but its weak resistance to ageing due to the unsaturation present in the chemical structure limits its applications.

To improve its durability, NBR is blended with various polymers, in particular with poly(vinyl chloride) (PVC), which is supposed to enhance the ozone and thermal ageing resistance and the mechanical properties of NBR. NBR/PVC blends are described as miscible, partially miscible or immiscible blends depending on the ratio of each polymer, the acrylonitrile content and the characterization technique [1–4].

Under use conditions for outdoor applications, cracks can appear at the surface of hoses made with NBR/PVC blends. The formation of cracks is an issue as they are a visible

consequence of the degradation and a loss of functional properties. Cracks have already been reported in papers dealing with ozonolysis in NBR/PVC blends [5], however this raises the question of the influence of UV-light in NBR/PVC blend degradation and the combined or not effect of photo- and thermooxidation of NBR/PVC blend to explain these different behaviours.

T. Skowronski *et al.* [6] studied NBR photodegradation at short wavelengths (λ < 254 nm) with NBR acrylonitrile contents varying from 21.7 to 41.6%. They showed the influence of the copolymer composition on the degradation of the material and highlighted that photooxidation occurred preferentially on the polybutadiene sequences, leading to the formation of carbonyl and hydroxyl species. For the study of photooxidation at long wavelengths (λ > 300 nm) of noncured NBRs, the same conclusions were shared by C. Adam *et al.* [7] and also by G. Scott *et al.*[8] in their study on photooxidative ageing of various blends based on polybutadiene. Studies on the thermal ageing of NBR have led to similar results [9–12]; F. Delor *et al*. [9] have shown that the CN bonds were not affected over the ageing time, while the double bonds were particularly affected and carbonylated and hydroxylated products were formed. The proposed degradation mechanism of NBR was then based on the polybutadiene degradation mechanism, which has already been the subject of many studies [13–15].

PVC photodegradation has already been reported [16–18]: it has been shown that it leads to the formation of conjugated polyene sequences by the loss of HCl (dehydrochlorination reaction) and the oxidations of these polyenes. The formation of ketones was also observed; due to their photochemical instabilities, leading to the formation of carboxylic acids. Other products are formed as chlorine radicals that are able to attack the polymeric chain. The main products observed by infrared spectroscopy are carboxylic acids, hydrochloric acid or even chlorocarboxylic acids. In conditions of thermooxidation, PVC only generates polyenes through the dehydrochlorination reaction, followed by the oxidation of these polyenes. The products are then saturated ketones, esters, peresters and lactones [18,19].

Different studies on polymer blends demonstrated that it was not possible to predict the degradation behaviour of blends from those of the homopolymers. Indeed, a stabilizing effect has been observed in some cases [20–22], whereas other studies reported that the degradation of one component leads to the degradation of the other one [23–26]. The photochemical behaviour of the NBR/PVC blend has been scarcely studied. T. Skowronski *et al.* [27] reported a study of the photodegradation of a PVC/NBR (90/10 wt%) blend and concluded that the formation of hydroxyl species was due to the butadiene unit of NBR, but the blend morphology influenced the degradation rate. A miscible blend with one phase was

reported to be less resistant to UV light, which was explained by the reaction of the free radicals that were formed in one polymer of the blend reacting with the other polymer, leading to its degradation.

In this paper, we focus on the degradation of a crosslinked NBR/PVC blend (65/33 wt%) under photo- and thermooxidation conditions. The aim was to put in evidence the links between the chemical structure changes induced by oxidation and those observed at the macromolecular scale and on the mechanical properties in order to explain how these modifications will lead to the occurrence of surface cracks.

2. Experimental

2.1. Materials

A commercial nitrile butadiene rubber (NBR) with a 33% acrylonitrile content and a Mooney viscosity of 45 and poly(vinyl chloride) (PVC) with kwert K > 60 were used. Curing agents were also added: sulfur and an accelerator, CBS (N-cyclohexyl-2-benzothiazolesulfenamide**)**. All products were provided by Trelleborg Industrie SAS.

The composition of the NBR/PVC blend is given in **Table 1**

Table 1. Composition of the NBR/PVC blend

(%wt)	NBR	PVC	Sulfur	CBS
NBR/PVC	65.3	32.7	1.3	0.7

2.2. Sample preparation

Blends were prepared at Trelleborg Industrie SAS in a Banbury mixer type. First, NBR and PVC were mixed at 50 rpm for 10 min at 160 °C. Then, the final batch was passed on a two-roll mill at 60 °C for 12 min with curative agents. No stabilizers were added for processing. Rheometric characterization was performed to determine the optimized vulcanization time using a moving die rheometer (Monsanto MDR 2000E) at 155 °C for 1 h, and it appeared that 30 min was needed to cure the samples. Therefore, 2 mm cured samples were made by compression moulding, and thin films (115 µm) were made by pressing uncured blends at 155 °C for 30 min under 200 bar pressure to obtain cured blends. Films with a thickness of 10 µm were obtained by microtomic sectioning of a 2 mm cured sample.

For micro-FTIR, thick films were immersed in liquid nitrogen and then placed in a Leica RM2165 microtome with a tungsten carbide blade inclined at 90°. The cross-section of the blend film was cut to a thickness (approximately 25 µm).

All the studied samples are cured blends and are further denoted as NBR/PVC blends.

2.3. Accelerated ageing and test conditions

A minimum of three films of the same sample were studied per ageing time to ensure good reproducibility.

2.3.1. Photoageing

Films were irradiated under artificial ageing conditions in a SEPAP 12/24 unit from Atlas (Ametek). It is equipped with polychromatic sources, which are four medium-pressure mercury lamps with borosilicate envelope filtering wavelengths below 295 nm. The irradiance was 90 W/m^2 in the range 295-420 nm, and the instrument setting of temperature at the surface of the sample was fixed at 60 °C (measured temperature: 54 °C) due to a PE film as the probe. Irradiation was carried out in the presence of oxygen (under air).

2.3.2. Thermal ageing

Films were thermooxidized in a forced air venting oven Memmert UF30 at a temperature of 120 °C. The oven temperature was controlled with a tolerance of ±1 °C.

2.4. Characterization techniques

2.4.1. UV–Vis spectroscopy

UV–Visible spectra of 115 µm thick films were recorded between 200 and 800 nm in a Shimadzu UV-2600 scanning photometer with an integrated sphere.

2.4.2. FTIR spectroscopy

Infrared spectra were recorded in transmission mode using a Thermo Scientific Nicolet 6700 spectrometer with Omnic Software. Spectra were obtained with 32 scans and a 4 cm^{-1} resolution. A minimum of three samples were analysed to obtain good reproducibility.

Infrared spectra in ATR mode were recorded using a Thermo Scientific Nicolet iS10 with a germanium crystal, a 4 cm^{-1} resolution and 32 scans. Data were studied with Omnic Software.

Oxidation profiles were obtained using a Nicolet Continµum microscope coupled to a Nicolet IS10 spectrometer (Thermo Scientific). Spectra were recorded every 5 µm with an aperture of 10 µm, with a 4 cm^{-1} resolution and 32 scans.

2.4.3. DMTA

To determine the dynamic mechanical properties of unaged and aged samples, a TA Instrument (Waters™) Q800 DMA was used. A liquid nitrogen tank was linked to reach low temperature (-50 °C). Two types of clamps were used:

- Tensile mode for thick films (e >100 µm). Rectangular samples of 1 cm x 1.5 cm x 135 µm were prepared for measurements.

- Single cantilever (SC) for thin films (e <20 µm). Stainless steel pockets (Mettler Toledo) were used. These envelopes do not have transitions; they allow us to follow thermal transition evolution but not modulus transition.

The temperature range was from -50 °C to 100 °C, and the heating rate was 3 °C/min at a fixed frequency of 1 Hz. The applied strain was 0.05% in tensile mode and 0.05% in SC mode.

A minimum of five samples were analysed to ensure good reproducibility for DMTA characterization.

The molecular weight between two cross-link points (M_c) can be calculated through the following Eq.1 using rubber elasticity theory [28,29]:

$$M_c = \frac{3\rho RT}{E'(T)} \qquad \textit{Eq.1}$$

where ρ is the density of the network at temperature T, R is the gas constant, and E'(T) is the rubbery modulus at temperature T = T_g+40 K in this study.

The equation 1 was established for unfilled elastomers, it is subjected to corrective models to be applicated to filled polymer. We used the equation based on Guth and Gold [30] model to calculate E'

$$E'(T) = \frac{E'(T)_{filled}}{(1 + 0.67\,\varphi f + 1.62\,\varphi^2 f^2)} \qquad \textit{Eq.2}$$

Where φ is the volume fraction of fillers (i.e. 0.36) and f is the shape factor (length/breadth), f=3 based on Sosson [31] work.

2.4.4. Swelling measurements

Tetrahydrofuran (THF) was chosen as the solvent for swelling measurements because NBR and PVC are both soluble in THF. After curing, the NBR/PVC blend swells, and the extent of the swelling depends on the crosslinking degree. A well-known mass of a sample (W_0) was put into THF at room temperature for 24 h. The swollen sample was then removed, wiped with tissue paper to remove excess solvent from the surface and weighed (W_s). Then, it was placed in an oven under vacuum at 50 °C for 24 h. The dried sample was further weighed (W_{ins}). The curative system used was chosen to crosslink the NBR phase, so the expression of swelling was adjusted to take into account the amount of PVC in the blend, based on Flory-Rhener swelling theory and Kraus rubber-filler interaction theory [28, 29]. The expression of the swelling ratio and the insoluble fraction are calculated as

$$Swelling\ ratio\ (Q) = 1 + \frac{\rho_1}{\rho_2} * \frac{W_s - W_{ins}}{W_{ins}(1-\varepsilon)} \quad \textit{Eq.3}$$

$$F_{ins} = 100 * (1 - \frac{W_0 - W_{ins}}{W_0(1-\varepsilon)}) \quad \textit{Eq. 4}$$

Where ρ_1 is the density of the polymer, ρ_2 is the density of the solvent, and ε is the weight fraction of the fillers.

As we assume that the PVC does not influence the crosslinking density, it becomes the following expression:

$$\upsilon = -\frac{V_{r0}}{V_s} * \frac{\ln(1-V_r) + \chi V_r^2 + V_r}{V_{r0}^{1/3} - \frac{V_{r0}}{2}} \quad \textit{Eq.5}$$

Where V_{r0} is the rubber volume fraction at the swelling equilibrium, which can be expressed as the inverse of the swelling ratio:

$$V_{r0} = \frac{1}{Q} \quad \textit{Eq.6}$$

And V_r is

$$V_r = \frac{\frac{W_{ins(1-\varepsilon)}}{\rho_1}}{\frac{W_{ins}}{\rho_3} + \frac{W_s - W_{ins}}{\rho_2}} \quad \textit{Eq. 7}$$

With ρ_3 the density of the blend.

The interaction parameter (χ) of NBR/THF is calculated by using Hildebrand model and the used value is 0.35.

$$\chi = 0.34 + \frac{V_s}{RT}(\delta_{THF} - \delta_{NBR})^2 \quad \textit{Eq.8}$$

Wherein δ_{THF} (i.e. 9.5 $(cal/cm^3)^{1/2}$) is the solubility parameter of solvent and δ_{NBR} (i.e. 9.57 $(cal/cm^3)^{1/2}$) is the solubility parameter of rubber.

Finally, it is possible to calculate the molecular weight between two crosslink points (M_c) thanks to the following equation:

$$M_c = \frac{\rho_2}{\upsilon} \quad \textit{Eq.9}$$

2.4.5. Thermoporosimetry

Thermoporosimetry analysis consisted of measuring the freezing point of THF contained in swollen NBR/PVC blends. The sample was placed into THF at room temperature for 24 h, removed and immediately analysed by DSC. The DSC procedure with a DSC instrument (Mettler Toledo 3+) was as follows: an isotherm at -150 °C for 5 min, then the temperature rate increased at 3 °C/min from -150 °C to 50 °C. The freezing point is directly linked to the crosslinking density, and it decreases as the system crosslinks. The relation used is [32]

$$T_p = A * T_0 + \frac{B}{R_p} \qquad \textit{Eq.10}$$

where T_p is the crystallization temperature of the solvent confined in a R_p radius pore and T_0 is the crystallization temperature of the free solvent.

2.4.6. Shore A Hardness measurement

Shore A hardness measurements were made with a Hildebrand durometer. According to the norme [ISO 48-4:2018], 6 mm thickness samples were used, and an average of 10 tests is given.

2.4.7. Atomic force microscopy

The peak force QNM mode in AFM was used to determine the mechanical properties of the NBR/PVC blend. Measurements were performed with a Brucker multimode 8 model with a nanoscope 9.20 in tapping mode. An RTESPA150 probe from Brucker with a curvature radius of 8 nm and a spring constant near 40 N/m was used.

Modulus measurement was performed on the exposed surface to monitor the stiffness evolution between aged and unaged material. Images of 5 µm x 5 µm at a scan rate of 0.5 Hz, and 512 scans were recorded. A minimum of 3 different sample zones were tested, and the average of the 3 images was taken. Probe calibration was realized with PDMS (3.6 MPa), but it was not enough to obtain quantitative measurement of the reduced Young modulus; therefore, the study is limited to the relative evolution of stiffness. The stiffness was evaluated thanks to the reduced Young's modulus E* obtained with DMT modulus images. The Derjaguin-Muller-Toporov model was used to determine the mechanical modulus.

3. Results and discussion

3.1. Chemical modifications

Infrared spectroscopy is widely used to monitor the oxidative ageing of various materials and is particularly sensitive to detect carbonylated species. Analysis of changes in the IR spectra first requires the identification of the absorption band of the NBR/PVC blend before ageing.

Figure 1 shows the IR spectrum of the NBR/PVC blend before ageing, and the attributes of the IR bands are given in Table 2.

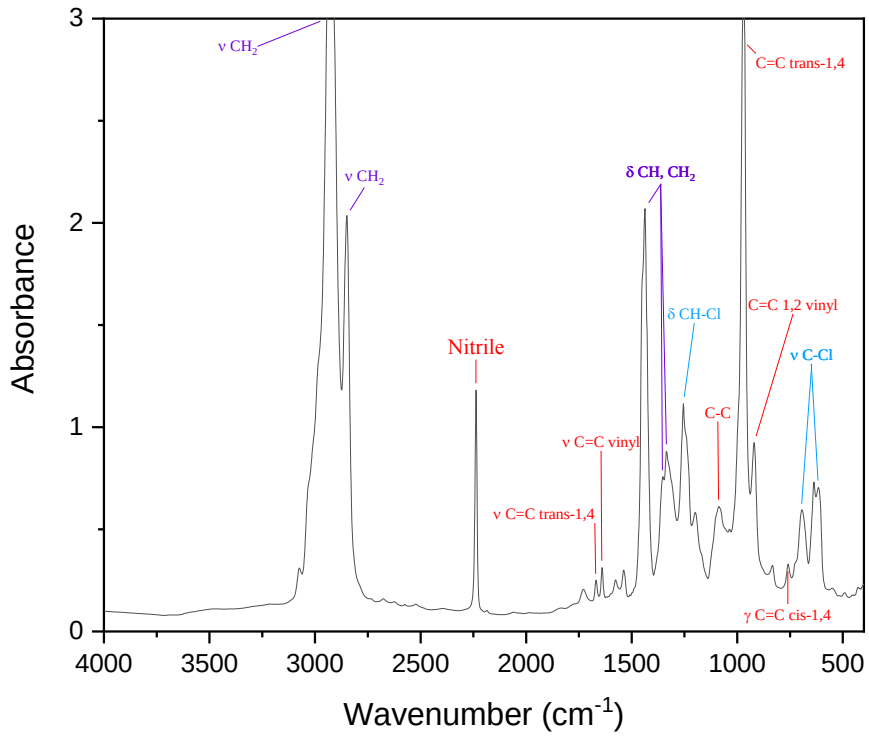

Figure 1. FTIR spectrum of NBR/PVC blend film (e= 115 µm) before ageing

Table 2. Attribution of Infrared absorption bands of the NBR/PVC blend

Wavenumber (cm^{-1})	Attribution		Ref
2940, 2850	Asymmetric/symmetric CH_2 stretching	NBR, PVC	[33,34]
2240	Nitrile (C-N)	NBR	[34]
1730	C=O stretching	NBR impurities	[34]
1668	C=C trans-1,4 stretching	NBR	[34]
1640	C=C vinyl stretching	NBR	[34]
1580, 1540	Stearates stabilizers	NBR impurities	[34]
1440, 1350, 1320	CH, CH_2 bending	NBR, PVC	[34]
1255	C-Cl bending	PVC	[35]
1070	C=C trans-1,4	NBR	[34]
966	C=C trans-1,4	NBR	[34]
920	C=C vinyl-1,2	NBR	[34]
730	C=C cis-1,4	NBR	[34]
690,615	C-Cl stretching	PVC	[35,36]

3.1.1. Photoageing

The photooxidation of the NBR/PVC film leads to modifications of the chemical structure monitored by infrared spectroscopy. Figure 2 shows the two main regions where changes occur. In the carbonyl region **(**Figure 2a), IR bands develop with an absorption maximum at 1715 cm^{-1} and shoulders at 1775 cm^{-1} and 1690 cm^{-1}. In the first hours of irradiation, an IR band at 1690 cm^{-1} appears but becomes difficult to observe after 10 h of irradiation. The hydroxyl region (Figure 2b) shows a broad absorption band with a maximum at 3490 cm^{-1} achieved during the first irradiation hours. Species at 3490 cm^{-1} correspond to products such as hydroperoxides, OH, and OH from acidic groups [7].

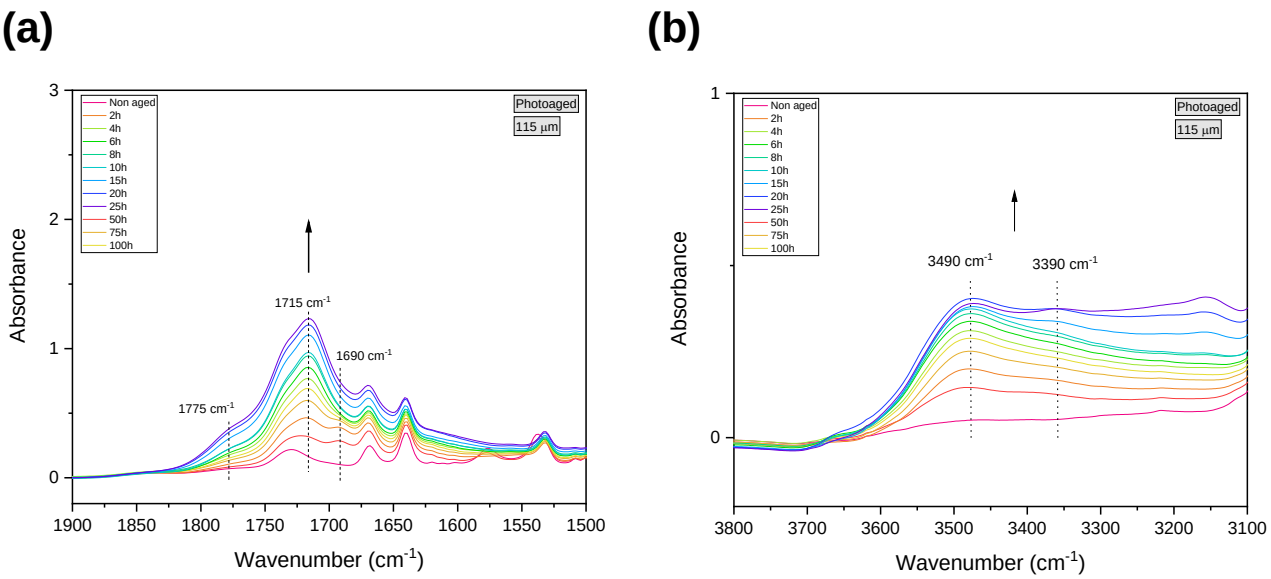

Figure 2. FTIR spectra of (a): the carbonyl region (1900-1500 cm^{-1}) and (b): the hydroxyl region (3800-3100 cm^{-1}) of the NBR/PVC film during photooxidation

During irradiation, there is no evolution of the IR absorption band assigned to the nitrile group (2240 cm^{-1}) of the NBR/PVC blend film, which means that acrylonitrile sequences are not involved, this result is in good agreement with the previous works of F. Delor-Jestin *et al.*[34] and C. Adam [7] about noncured NBR..

To follow the modifications of the unsaturations of NBR/PVC, ATR-IR spectra were also monitored.

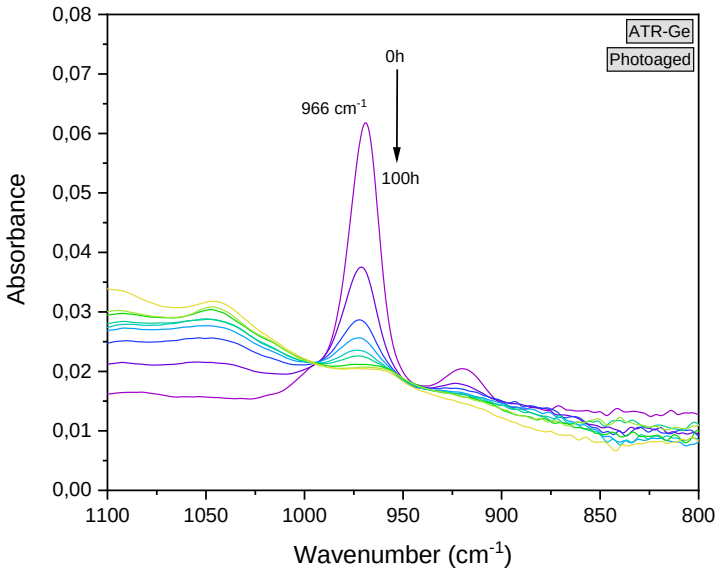

Figure 3. ATR-FTIR spectra of the NBR/PVC blend during photooxidation in the 1100-800 cm^{-1} region

Figure 3 shows a magnified view of the 1100-800 cm^{-1} region of the IR spectra obtained by ATR-Ge to monitor the evolution of the 920 cm^{-1} and 966 cm^{-1} absorption bands assigned to 1,2 vinyl and 1-4, trans double bonds, respectively. A decrease is observed corresponding to the consumption of unsaturations linked to the butadiene part of the polymer [7,14,15,37].

We have also compared subtracted spectra of PVC, NBR and NBR/PVC blend films photooxidized 100h in terms of oxidation products. A particular attention was given to the carbonyl region (1900-1500 cm^{-1}) represented in Figure 4.

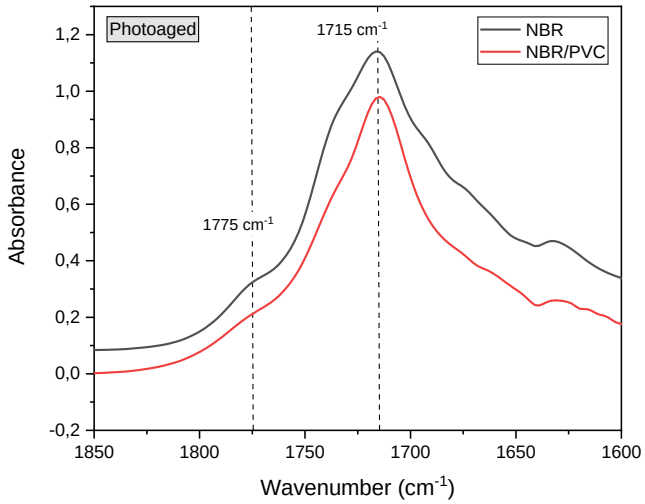

Figure 4. Subtracted IR spectra of NBR and NBR/PVC films in the region 1850-1600 cm^{-1}

We can note that the maximum of the broad IR band is at 1715 cm^{-1} and a shoulder at 1775 cm^{-1} is observed for NBR and the NBR/PVC blend. No band is observed at 1745 cm^{-1} for the NBR/PVC blend (the oxidation IR band reported for PVC [16]). The absorbance of carbonylated products for NBR/PVC is similar to that for NBR, for a same ageing time. This shows no influence of PVC on the photooxidation of NBR, in the NBR/PVC blend, and the degradation mechanism of NBR/PVC is comparable to that of neat NBR. To complete this study, degradation of a NBR/$CaCO_3$ blend was also performed. The spectra and the associated absorbance variation are given in supporting information (Figure S1). This result shows no influence of $CaCO_3$ on the photooxidation of NBR in the blend. Moreover, no difference was observed between the NBR , NBR/PVC and NBR/ $CaCO_3$ blends during the exposure duration. Therefore, PVC in the blend has been considered as a diluent.

Studies on the photooxidation of NBR have shown that the weak point of this copolymer is the butadiene units, which also seem to be the initiating point for the degradation of the NBR/PVC blend. Photooxidation of polybutadiene (PB) has received much attention in the literature, and the mechanism was described as a radical chain mechanism [6,37–39]. Under the effect of an energy source, the defects present in the NBR (impurities, structural defects) could form radicals. As summarized in Figure 5, the initial stage is the primary radical attack on the C-H bond in the α-position to the double bond (966 cm-1 for 1,4 trans and 920 cm-1 for 1,2 vinyl), leading to alkyl formation. In the presence of oxygen, alkyl radical ($P^{\bullet}$) reacts to form peroxyl radical ($POO^{\bullet}$) which becomes hydroperoxides (POOH) after abstraction of a hydrogen atom from the macromolecular chain. Hydroperoxides (POOH) decompose under irradiation or high temperature to give two radicals: alkoxyl ($PO^{\bullet}$) (I) and hydroxyl ($HO^{\bullet}$) (II) radicals, as represented in Figure 5.

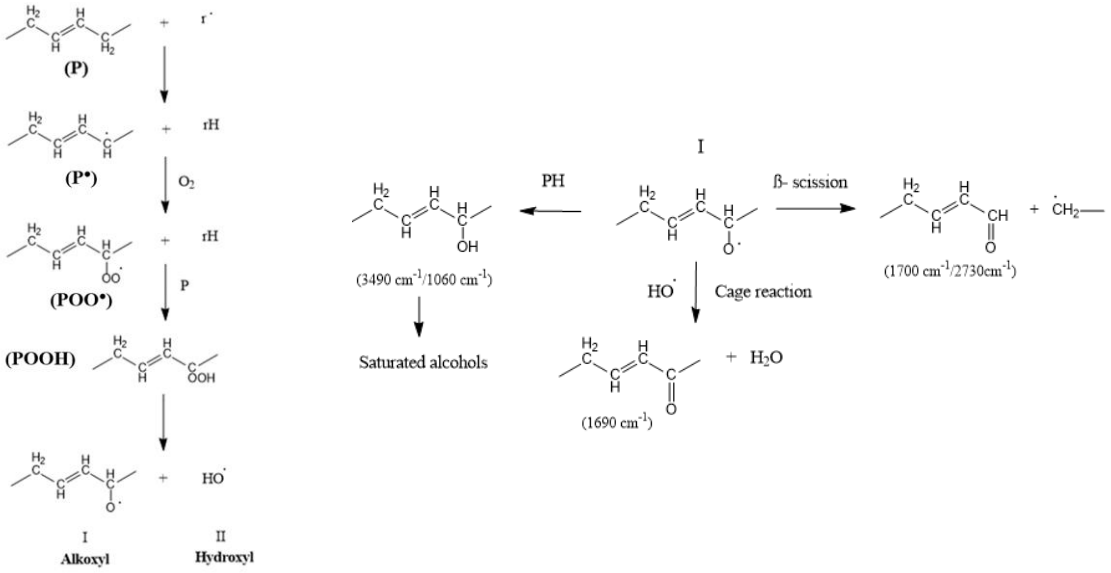

Figure 5. Mechanism of oxidation of butadiene sequences in NBR

Alkoxyl radical (I) reacts to form:

- α, β-unsaturated alcohols (at 3490 cm^{-1}) by labile hydrogen attack [7]. After oxidation, unsaturated alcohols lead to saturated alcohols.
- α, β-unsaturated ketones from the cage reaction of the alkoxyl radical with hydroxyl radical ($HO^{\bullet}$) are detected at 1690 cm^{-1}. Ketones are not photostable; they decompose through Norrish reactions and lead to saturated carboxylic acids (at 1715 cm^{-1}).
- Unsaturated aldehydes by β-scission. After oxidation, unsaturated aldehydes are converted to saturated aldehydes and carboxylic acids (1715 cm^{-1}).

At the same time, crosslinking reactions occur;

- either by reaction of the alkoxy radical (I) on a double bond, leading to an ether bridge between the macromolecular chains,
- and/or by reaction of the alkyl radical ($P^{\bullet}$) on a double bond creating a C-C bridge between the macromolecular chains.

The shoulder at 1775 cm^{-1} could be γ-lactones obtained by two hydroperoxides cyclization, anhydride formed by dehydration of carboxylic acids, and/or peresters [15].

Rate of photooxidation

The variation in the absorbance of the IR bands (at 1715 cm^{-1} and 3490 cm^{-1}) was plotted as a function of the irradiation time to characterize the oxidation kinetics of the NBR/PVC blend. Figure 6a shows no induction time for these two bands with a huge increase in absorbance observed between 0 and 25 h of irradiation. After 50 h, these absorbances reach a plateau.

These phenomena have already been observed in other studies [13,15] in the case of an oxidation profile within the material. This profile is usually observed in rubber materials because of the heterogeneous degradation coming from either a decrease in the oxygen permeability due to a crosslinking reaction or a light absorption profile [7,13,40].

The decrease in IR bands of unsaturations was studied in transmission mode for the band at 920 cm^{-1} and in ATR-Ge mode for the band at 966 cm^{-1} because of the too-high absorbance of the latter in transmission mode (i.e., Beer–Lambert law). Figure 6b shows that the band at 920 cm^{-1} corresponding to 1,2-vinyl double bonds follows the same trend as the one at 966 cm^{-1} because, as shown in the mechanism, radicals can react with both kind of double bonds and lead to crosslinking. There is a large decrease during the first hours, and a plateau is reached after 25 h to 50 h for these both bands, as observed for the IR bands at 1715 and 3490 cm^{-1}(Figure 6).

a) **b)**

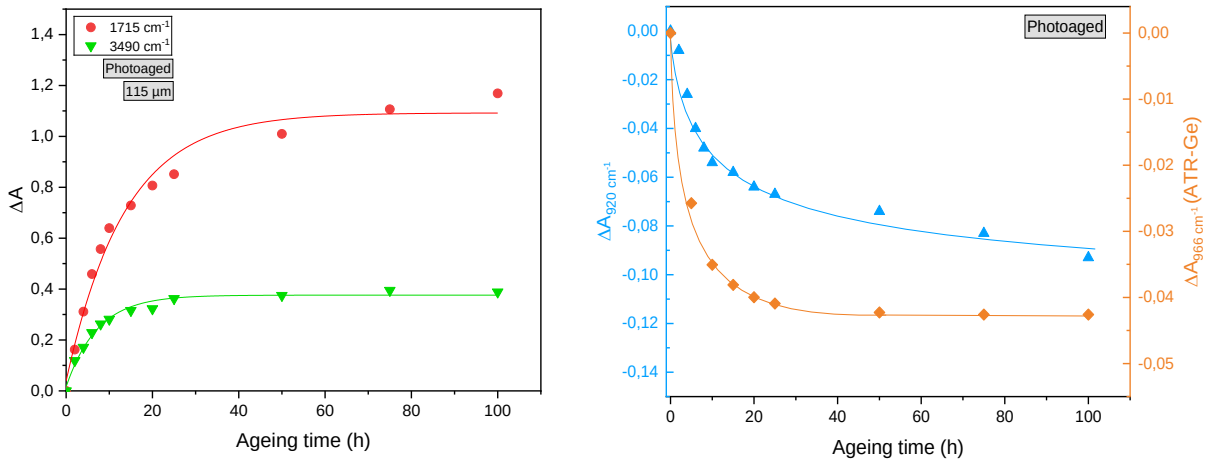

Figure 6. Absorbance variation at (a): 1715 cm^{-1}(●) and 3490 cm^{-1}(▼) and (b): 920 cm^{-1}(▲) and 966 cm^{-1}(♦) during photooxidation for a NBR/PVC film

3.1.2. Thermal ageing

Thermal ageing of the NBR/PVC blend was performed at 120 °C, and chemical modifications were followed by IR spectroscopy (Figure 7).

During thermoooxidation, the IR spectra of the NBR/PVC blend film show the formation of the same IR bands as those observed in photooxidation, with a maximum at 3490 and a shoulder at 3370 cm^{-1} for the hydroxylated species (Figure 7a) and a maximum at 1715 and 1690 cm^{-1} and a shoulder at 1775 cm^{-1} for the carbonyl product (Figure 7b). Under thermoooxidation conditions, there was also no significant change in the absorbance of the IR band of the nitrile group (at 2240 cm^{-1}), as mentioned in previous work [9].

It was reported that thermoooxidation of NBR followed the same degradation pathways as photochemical ageing [9,11,12,41–43], and the main oxidation products were identified: alkoxyl and hydroxyl radicals are formed and lead mainly to the formation of alcohols (3490 cm^{-1}), lactones (1775 cm^{-1}), saturated carboxylic acid (1715 cm^{-1}) and ketones (1690 cm^{-1}).

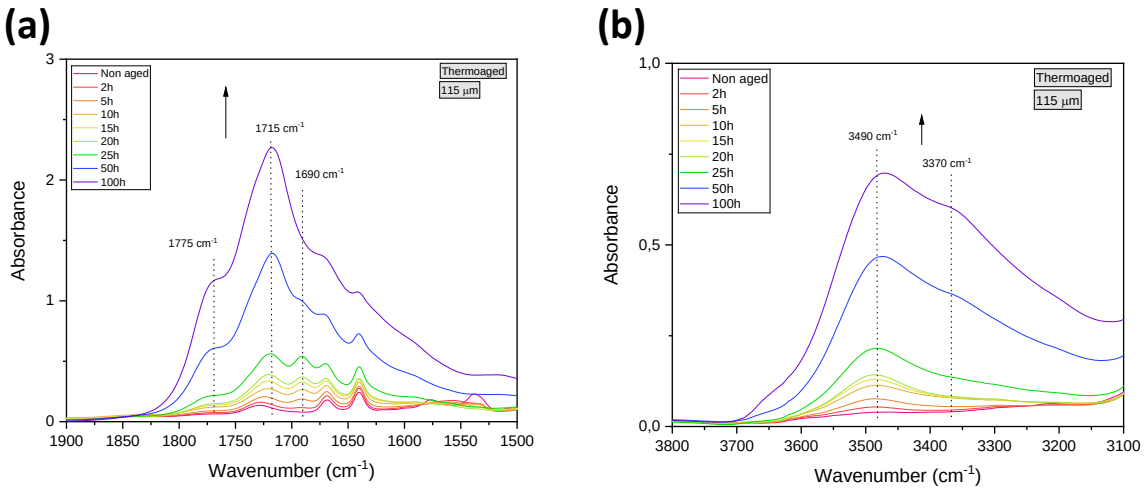

Figure 7. FTIR spectra in (a): the carbonyl region (1900-1500 cm^{-1}) and (b): the hydroxyl region (3800-3100 cm^{-1}) of the NBR/PVC film during thermooxidation

Rate of thermoooxidation

Figure 8 displays the variation in the absorbance of the IR bands (at 1715 and 3490 cm^{-1}) as a function of the irradiation time. The curves show two different periods as the slope changes after 25 h with an increase in the kinetic rate. The first period corresponding to a slower process can be due to the presence of a residual processing antioxidant. We do not observe a plateau up to 100 h, which suggests that there is no oxidation profile, in contrast to the case of photooxidation (see Figure 6).

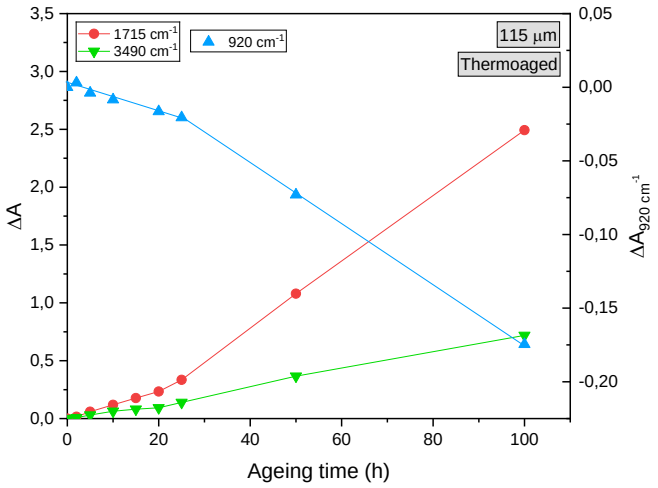

Figure 8. Absorbance variation at 920 cm^{-1} (▲), 1715 cm^{-1} (●) and 3490 cm^{-1} (▼) during thermoooxidation for a NBR/PVC film

Photooxidation versus thermoooxidation

If we compare the IR spectra of photo- and thermooxidized NBR/PVC films, we observed that the same IR bands appeared but with different stoichiometries. Figure 9 shows the subtracted IR spectra (between aged samples and the nonaged samples) for NBR/PVC films after either 4 h of photooxidation or 25 h of thermoooxidation. We can observe that for the same absorbance (A = 0.5) for the band at 1690 cm^{-1}, the absorbances for the two other bands at 1715 and 1775 cm^{-1} are different. The oxidation product corresponding to the IR band at 1715 cm^{-1} is formed in lower amount in the case of thermoooxidation compared to photooxidation, whereas the product corresponding to the IR band at 1775 cm^{-1} is formed in higher amount in thermoooxidation than during photooxidation. From the proposed mechanism, these oxidation products developing at 1690 cm^{-1} would be ketones, which would be consistent with their photochemical instability, and then they are not present (or are present to a lower extent) in photooxidation. In addition, the shoulder at 1775 cm^{-1} is much more pronounced for the thermooxidized NBR/PVC blend. However, the mechanism of oxidation of PB cannot explain this difference. Knowing that PVC is particularly poorly resistant to thermal degradation, we can reasonably assume that it can be a product of PVC degradation.

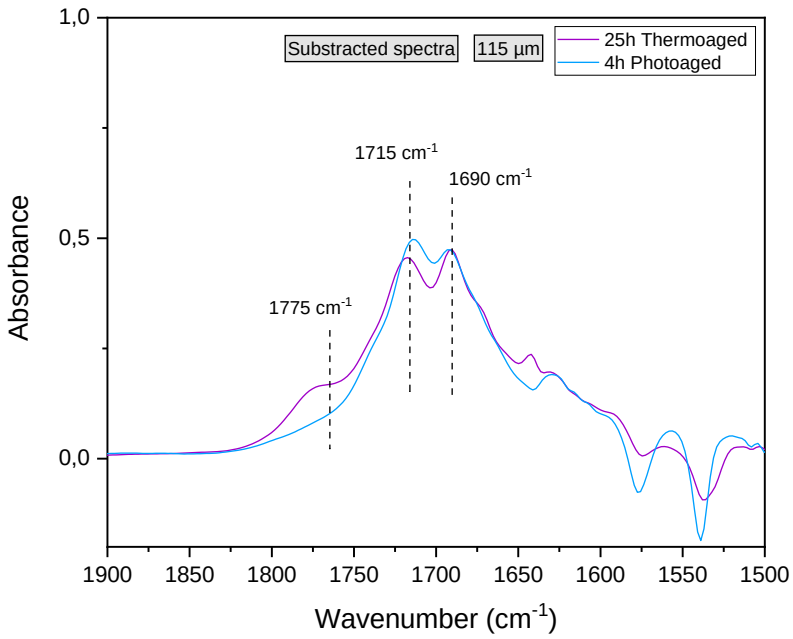

Figure 9. Subtracted spectra between the nonaged and aged NBR/PVC film (after 4 h photooxidation and 25 h thermooxidation)

UV-visible spectrum and light absorption profile

Figure 10a displays the UV-visible spectrum of a NBR/PVC film before ageing. We observe a high absorbance value at 400 nm for a film of 115 µm thick; revealing the yellow colour of the blend. This can be attributed to sulphurous species used to cure the polymer. It is also important to note that no evidence of the presence of dienes specific of the PVC aging have been monitored during all the exposure duration.

(a) **(b)**

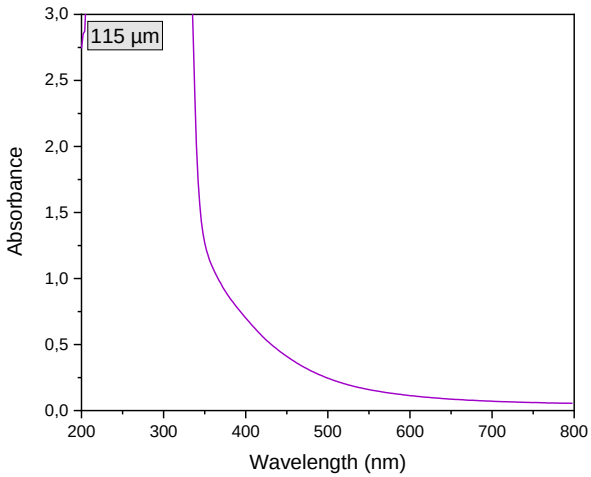

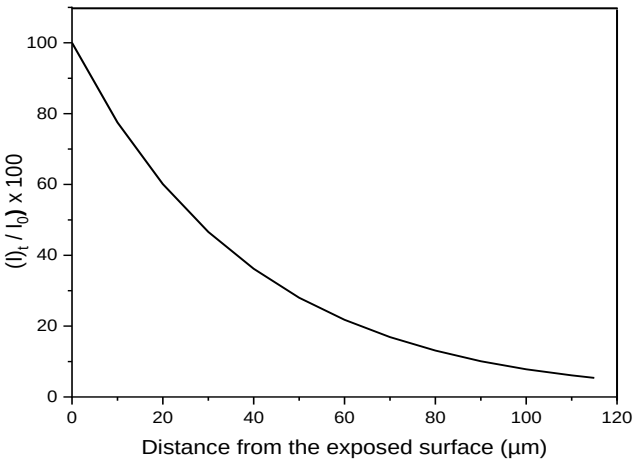

Figure 10. (a): UV–visible spectrum (b): % of light transmitted at λ = 350 nm as a function of the distance from the exposed surface for a NBR/PVC film plotted from (a)

From the UV–visible absorption spectrum of an NBR/PVC film, we can plot the percentage of transmitted light / incident light (I_t/I_0 x100) at 350 nm as a function of the distance from the exposed surface (Figure 10b). The profile of light transmitted indicates that the UV light penetration (λ < 350 nm) is heterogeneous and that practically no light is absorbed after the first 80µm from the exposed surface (I_t/I_0 = 0.13 at 350 nm).

Oxidation profile

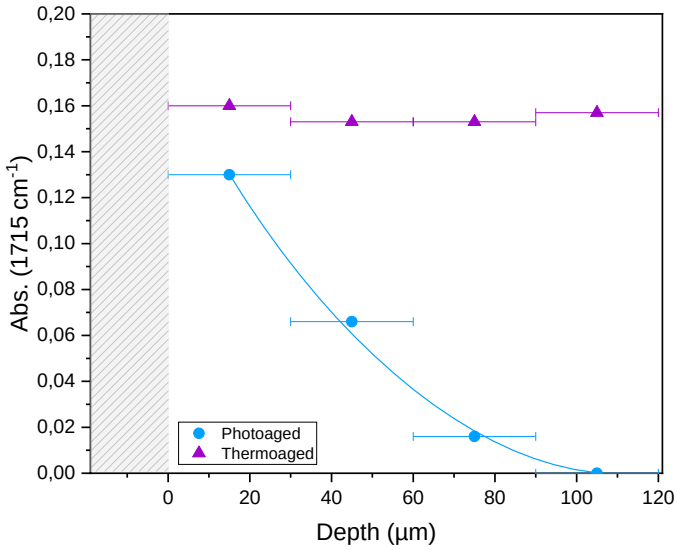

Figure 11. Changes of 1715 cm^{-1} absorbance in function of the depth (µm) after 100h of photooxidation

Measurements of absorbance at 1715 cm^{-1} were performed using an infrared microscope on microtomed aged samples (Figure 11) from the exposed surface to the bulk. In the case of photooxidation, the resulting absorbances at 1715 cm^{-1} of irradiated sample are highly different depending on the depth in the film; Figure 11 shows that there is an oxidation profile resulting in a heterogeneous distribution of oxidation products in the film thickness. This helps to explain the shape of the kinetic curves in Figure 6 with the formation of a plateau. Indeed, in the photooxidized film, two zones are distinct: the first microns of the exposed face are strongly oxidized, but the core of the film remains unmodified. Oxidation is superficial due to the limited UV-light absorption across the film depth as shown in Figure 10. In addition, one can also assume that the oxidation profile can be correlated to a decrease in the oxygen permeability, as previously reported by Adam *et al*. [7], crosslinking reactions and the formation of a network or densification of the network can lead to a profile. In the

thermooxidized film, if we compare the absorbances at 1715 cm^{-1} observed for the surface and the core, they are similar, which means that oxidation is homogeneous in the whole thickness of the film. This is in agreement with the kinetic curves obtained in Figure 8 under our accelerated ageing conditions. However, an oxidation profile, as previously described by Celina et al. [41], could have been recorded if the same study had been performed using a thicker film.

3.2. Macromolecular architecture modifications

This section of the paper is devoted to the characterization by DMTA and swelling measurements of changes at the macromolecular scale resulting from chain scissions or crosslinking reactions after polymer ageing [2,44–47].

3.2.1. Swelling measurements

Swelling ratio was measured on both thermo and photooxidized NBR/PVC blend films, and Figure 12a displays the swelling ratio as a function of time.

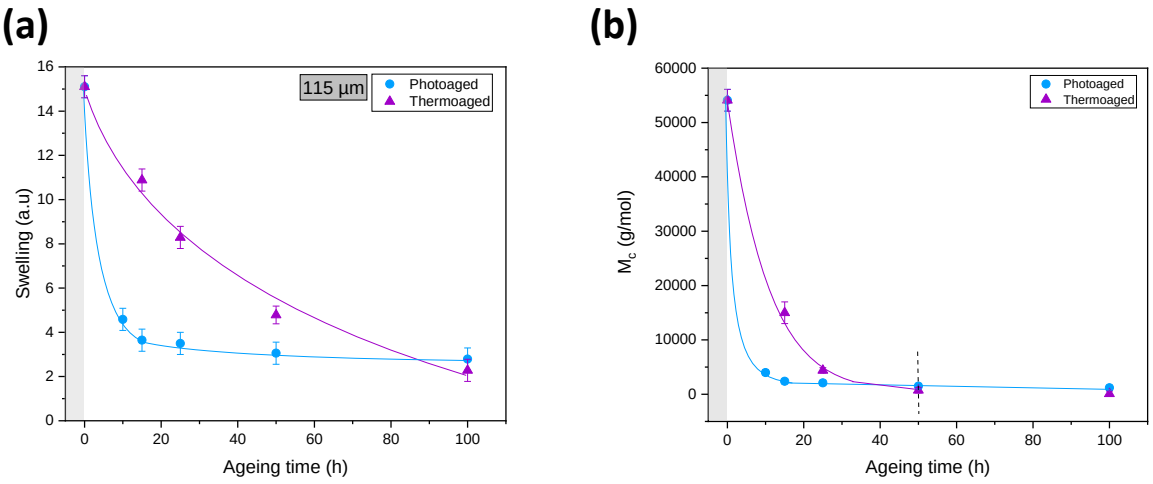

(c)

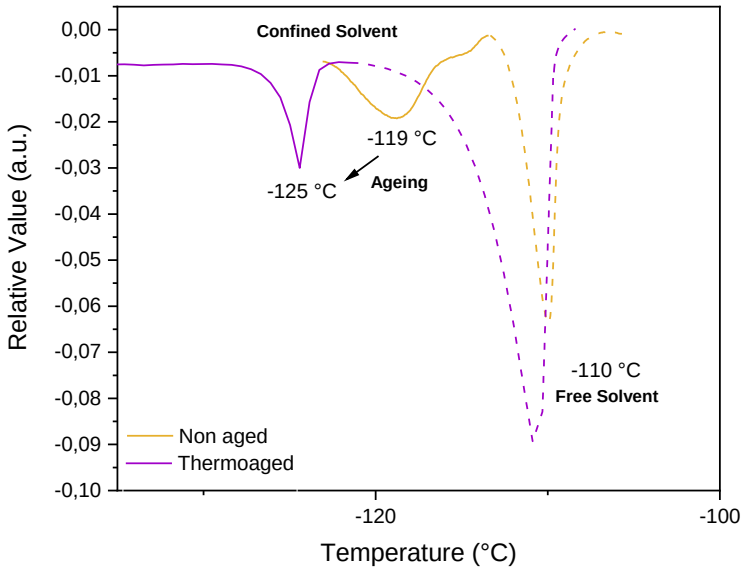

Figure 12. (a): Swelling ratio and (b): M_c variation of NBR/PVC film versus ageing time and (c): thermoporosimetry curves of NBR/PVC film before and after 200 h of thermoooxidation

For the photooxidized film, the swelling ratio sharply decreases in the first 10 hours of irradiation and reaches a constant value after 20 h. During thermal ageing, the swelling ratio decreases progressively and reaches a similar value as in photooxidation conditions after 80 h of ageing. From the swelling values, M_c of the NBR/PVC blend can be calculated using *Eq.**9*** and is given in Figure 12b. The same trends are obtained for M_c values as those reported for the swelling ratio. The decrease in molecular weight between two crosslink points (M_c) means that the mesh size of the network decreases upon ageing. These results reveal a network density phase from macroradical recombination in the presence of oxygen, as was also observed by S. Berthumeyrie *et al*. [48].

In addition, when a polymer is crosslinked, there is an insoluble fraction that can be characterized by swelling measurements when immerged in the appropriate solvent. For NBR/PVC blends, the vulcanization system reacts with the elastomeric part of the blend, that is the NBR part, while PVC would be able to be extracted by THF. Initially, the soluble fraction was calculated as $1\text{-}F_{ins}$ (Eq. 4) and represents 20% ± 5% which is less than the weight fraction of PVC in the blend. After ageing, we did not measure any soluble fraction, which means that PVC could be grafted or entangled. Based on N.R. Manoj *et al.* previous work [46], a crosslinking reaction between NBR and PVC can occur but the system needs a high temperature or light radiation leading to the dehydrochlorination of PVC with the formation of HCl. HCl could then react with NBR nitrile groups to form amines or acids and the active sites of PVC crosslinked with these groups. We did not observe any evidence of this reaction by infrared and UV-visible spectroscopies, which are the classically used

techniques to monitor this behaviour. In addition, swelling measurements do not seem satisfactory to claim there is a reaction between NBR and PVC as experiences reported on PVC/PB blend [25] gave the same result.

For the photooxidized NBR/PVC film, the swelling and M_c changes upon irradiation are similar to those obtained from kinetic curves obtained by IR analysis. The rate change occurs after the first 20 hours, which suggests a correlation between the consumption of double bonds and the network densification resulting from crosslinking. From photooxidation profiles (Figure 11), we have shown that oxidation occurred only at the irradiated surface in the case of the photooxidized film, meaning that the swelling ratio reached a limited value when the plateau in the consumption of double bonds was reached (see Figure 6). As thermooxidation is not limited to this superficial layer at this sample thickness, this explains why there is a constant decrease and no plateau in the swelling curve (Figure 12a). During the first hours of thermoooxidation, it is observed that the swelling ratio linearly decreases until 20 h. For longer ageing time, the swelling ratio is nearly impossible to measure because of extreme densification of the polymer network. Indeed, the amount of solvent that can penetrate the polymer network is so weak that it leads to meaningless measurement of the swelling ratio by the gravimetric method. This behaviour explains the evolution of the critical mass M_c (Figure 12b), which almost reaches zero at the end of both ageing processes. Usually, to overcome this detection limit, we complete the measurements by thermoporosimetry because it allows us to characterize the network density.

To better characterize the network modifications, thermoporosimetry experiments were then performed on these NBR/PVC films. Thermoporosimetry allows the network mesh size to be assessed by comparison to the pore size of a porous solid.

We did not obtain convincing results for the photochemically aged specimens, which might be explained by the oxidation profile and the degradation that is limited only to the surface. In the case of photooxidized films, small pores were formed but in a too small amount to be characterized. For the thermooxidized films, thermoporosimetry curves are presented in Figure 12c, showing that two separate peaks are observed when analysing the unaged NBR/PVC blend: one peak at -110°C corresponding to the free solvent, which appears at the melting temperature of THF, and a second peak at -119°C corresponding to the confined solvent. The confinement of the solvent causes a shift of its transition temperature to lower temperature. This shift is directly linked to the size of the mesh where the solvent is confined. Concerning the free solvent, the peak is similar for the unaged blend and the thermooxidized blend (at -110°C). For the confined solvent, before ageing, we can distinguish a broad peak

with a maximum centred at -119 °C and made up of two populations (bimodal). This suggests that in the initial state, the network after vulcanization is not homogeneous and is constituted of several mesh sizes. After thermooxidation, the peak of the confined solvent is at -125°C, showing a decrease in the transition temperature of the confined solvent. This results in a smaller pore size, and therefore indicates that crosslinking of the network occurred upon thermooxidation. The shape of this peak is symmetric, with no shoulder, meaning that there is only one pore size population, this would be consistent with a more homogeneous network in the thermooxidized blend. This result is consistent with those of swelling measurements and the densification of the polymer network upon thermoooxidation [32].

3.2.2. DMTA analysis

DMTA characterization was performed on NBR/PVC films before and after both kinds of ageing: under irradiation or thermal ageing. The effect of ageing on the loss tangent (tan δ) of the NBR/PVC blend is shown in Figure 13, and the T_g values of the NBR/PVC blend and their respective homopolymers (PVC and cured NBR) before ageing are reported in Table 3.

Table 3. Tg value of cured NBR, PVC and NBR/PVC blend. Calculated Tg from the Eq.11

	T_g value (K)	**Calculated T_g (K)**
Cured NBR	271	-
PVC	373	-
NBR/PVC blend	285	298

The NBR/PVC blend shows a single glass transition peak (Figure 13). The glass transition peak provides information about the miscibility of the blend; when a blend is miscible, its Tg value is supposed to be between the T_g value of the two components according to Fox's relation (Eq.11) [49]

$$\frac{1}{T_g} = \frac{w_1}{T_{g1}} + \frac{w_2}{T_{g2}} \qquad \textit{Eq.11}$$

where w_i is the weight fraction and T_{gi} is the glass transition temperature of blend component i.

In the case of the NBR/PVC blend, as we observe only one transition, we can consider that it is a miscible blend. Fox's law gives a theoretical glass transition temperature of T_g (NBR/PVC) = 25 °C (298 K), calculated from the values of the glass transition temperatures

of NBR and PVC obtained by DMTA, as indicated in Table 3. The value of T_g measured for the NBR/PVC blend is 12 °C (271 K). This value is between those of the two components of the mixture, and even if it does not perfectly follow Fox's law because of various factors, we can reasonably assume that NBR/PVC is a miscible blend, which is consistent with the literature [1]. Moreover, no other analysis has shown the presence of two distinct phases.

Thick films (115 µm) were analysed in tensile mode Figure 13a indicates that during photooxidation, there is a rapid decrease in the tan δ maximum value but no change in temperature, which means a decrease in the molecular mobility. For the thermooxidized NBR/PVC blend (Figure 13b), this decrease in the tan δ value is accompanied by a shift of the tan δ peak to higher temperatures, which can be identified as an increase in the glass transition temperature (T_g), and one can also see a broadening of the peak. This increase in the T_g value implies that the required energy for the transition is higher after thermoooxidation. The broadening of the tan δ peak reveals that the molar mass distribution is broader since the mid-height width of the tan δ peak is correlated to the polymer polydispersity. It is important to note that the tan δ peak is shifted to a higher temperature corresponding to a constant increase in the molecular weight, i.e., this behaviour is characteristic of many crosslinking reactions. All these changes result in embrittlement of the NBR/PVC blend.

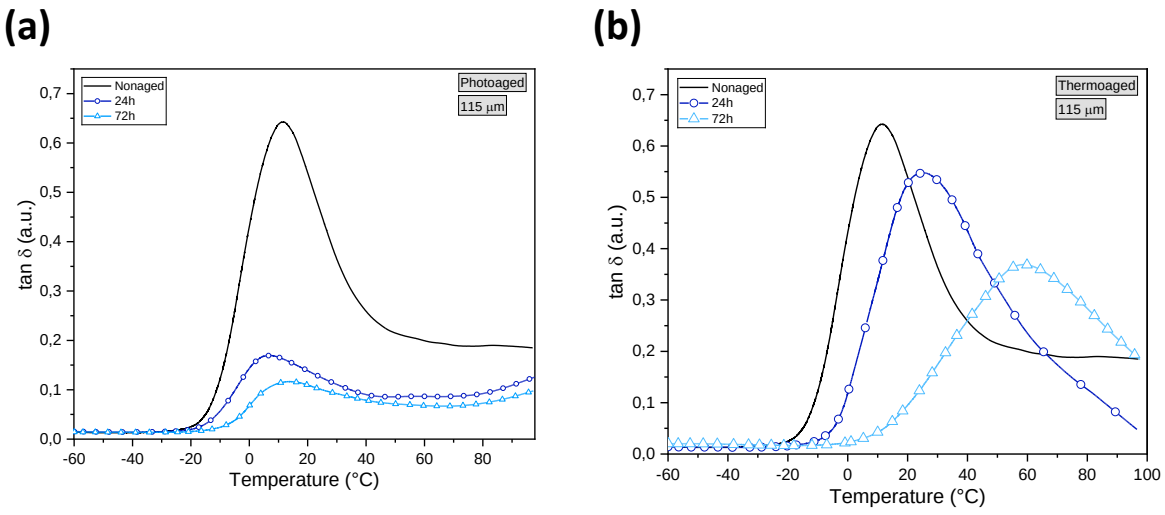

Figure 13. Tan δ variation of NBR/PVC blends before and (a): after 24 h photooxidation or (b): after72 h of thermoooxidation

In the case of photooxidation, as oxidation was shown to only occur in the first microns of the exposed face of the film, experiments on NBR/PVC films 10 µm thick (Figure 14) were also carried out in single cantilever mode because of the restrained thickness. The aim was to

study the glass transition temperature value and its evolution during photooxidation based on the extreme surface of the material, which presents different properties from the bulk. Under irradiation conditions, Figure 14 shows a shift in the T_g value to higher temperatures, indicating that crosslinking reactions occurred. This shift was not observed in the case of thicker films (Figure 13a) due to the existence of an oxidation profile, as previously shown.

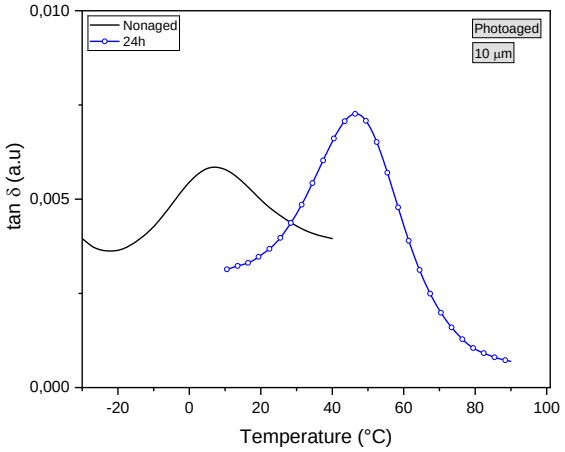

Figure 14. Tan δ variation of a 10 µm thick film of the NBR/PVC blend before and after 24 h of photooxidation

Using DMTA analysis and swelling measurement for thermoooxidized samples, it is possible to calculate an average of Mc. It is important to note that obtained quantitative value of Mc can be directly calculated from the storage modulus, but a quantitative determination requires a well-characterized sample, the DMTA apparatus should be perfectly calibrated. The interactions between the two polymers have to be correctly accounted for and the most appropriate model chosen. When all these requirements are met, the data still contained a rather large uncertainty and so in this paper the values of M_c that will be calculated and provided must be taken with caution. As a consequence, only the variations corresponding to the M_c (expressed in g/mol) are discussed in the next part. DMTA and swelling ratio can be considered as versatile tools for characterizing the crosslinking of polymers. We considered that the NBR/PVC blend was a miscible blend. However, we only observe the degradation of NBR in the studied time scale of ageing and not that of PVC. PVC can then be considered, for this specific study, as a diluent. Thus, to compare the changes in the mechanical properties with the ageing times, all the modulus and Mc values have been corrected in this way.

Mc values were calculated from Eq.1 and Eq.9 and reported in Table 4.

Table 4 - Mc value calculated for a thermooxidized NBR/PVC blend from DMTA analysis and swelling measurement

	from DMTA analysis (g/mol)	from swelling measurement (g/mol)
Ageing time (h)	Guth & Gold (eq.1&2)	Kraus (eq.10)
0	45 000	54 000
50	3 000	4 000

Using the equations mentioned in Section 2.4, the critical masses between two crosslink points for a thermooxidized NBR/PVC film were calculated. This allowed us to make a comparison of the results obtained by different analytical techniques (Table 4). It is important to note that NBR/PVC degradation leads to a severe decrease in M_c in both cases corresponding to crosslinking of the blend, one can see a drop of the M_c by an average factor of 9 after 50h of ageing and this independently of the used techniques. We can note that DMTA analysis gives M_c values in the same order of magnitude than those obtained by swelling measurement.

3.3. Degradation of functional properties

Characterization of surface properties was performed by shore A hardness measurements and AFM to highlight modulus variation during both kinds of ageing.

3.3.1. Shore A Hardness

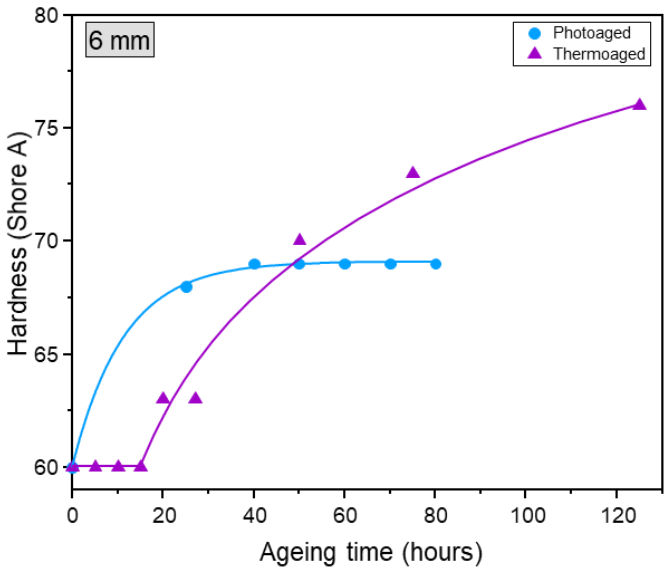

Figure 15. Shore A hardness variation versus photo- (●) and thermal (▲) ageing time

Figure 15 displays the shore A hardness as a function of ageing time for NBR/PVC thick samples either upon irradiation or thermal ageing. The hardness curve of the photooxidized NBR/PVC blend in Figure 15 has the same shape as the kinetic rate of formation of oxidation products in Figure 6: the surface stiffens rapidly in the first 20-25 h before reaching a plateau. This is consistent with what was already observed; the detected changes in the properties of the NBR/PVC blend are limited to the surface due to an oxidation profile. In contrast, the hardness of the thermooxidized NBR/PVC blend does not evolve during the first 20 h and then increases until 120 h of thermal ageing. Modifications are then only detected after approximately 20 h, this might be due to the too small variations occurring in the first hours. The hardness begins to evolve after 25 h of ageing, corresponding to the time after which we also observed a change in the slope of the oxidation rates in Figure 8 and the first variations in the molecular weight between two crosslinking points (M_c value) in Figure 12b or in the glass transition in Figure 13a.

The hardness modifications are consistent with the results reported above in this paper, a T_g increase of the NBR/PVC blend during ageing, meaning a densification of the polymer network. The denser the polymer becomes, the higher its surface hardness becomes. We can conclude that the consequences of the crosslinking reactions predominate for the evolution of the properties in both photo- and thermoooxidation.

3.3.2. Surface Aspect and DMT Modulus

Atomic force microscopy modulus mapping at the nanoscale was carried out on NBR/PVC blend samples before and after ageing to monitor stiffness changes. Images show differences for the aged samples. It can be seen in Figure 16b,c that after 100 h of ageing under photooxidation and thermoooxidation conditions, the surface roughness was modified, and in the case of photooxidation, cracks appeared after 100 h of irradiation. AFM gives an elastic modulus average value of 49 ± 1 MPa before ageing versus an average value of 132 ± 1 MPa after photooxidation and 172 ± 1 MPa after thermoooxidation. It reveals a gain in modulus of 185% and 274%, respectively, with an even more important increase after thermoooxidation. This confirms that the NBR/PVC blend becomes harder at the surface during both ageing processes because of crosslinking reactions.

(a) **(b)** **(c)**

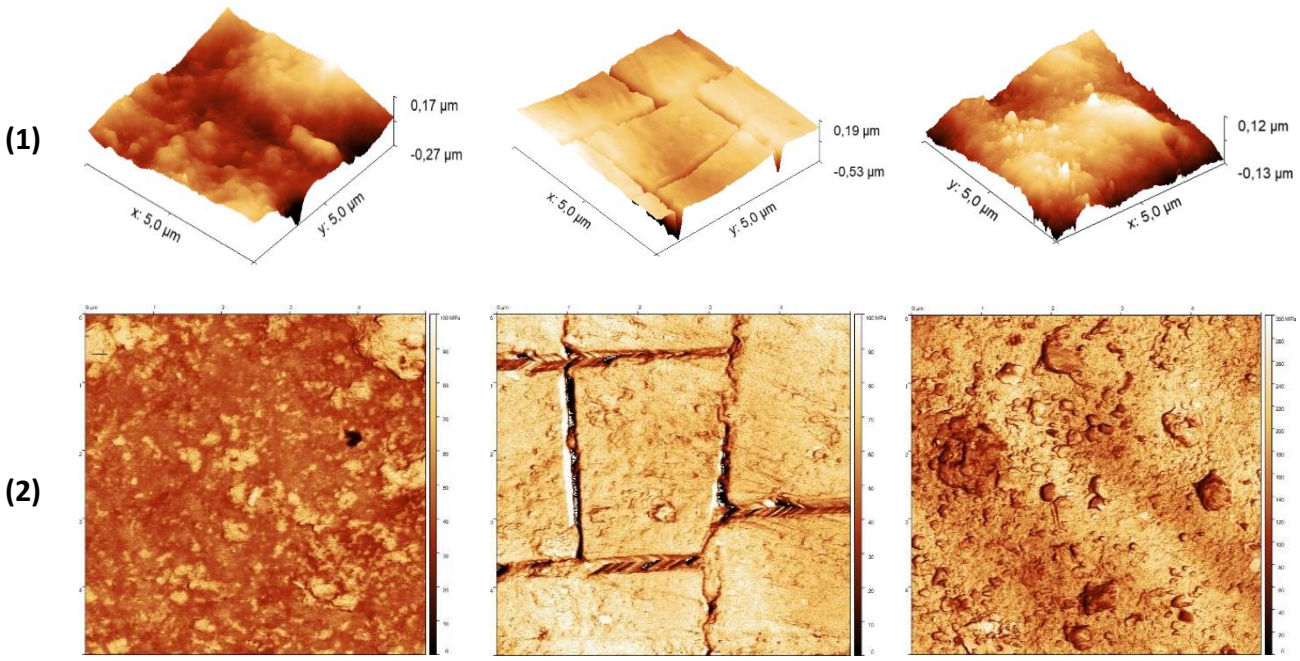

Figure 16. AFM topography images (1) and modulus images (2) of NBR/PVC blend (a): before ageing, (b): after photooxidation (100 h), (c): after thermoooxidation (100 h)

The occurrence of cracks during the photochemical ageing of elastomers is a consequence of the observation made at the structural and macromolecular scale because it is conditioned by the presence of oxygen. Its diffusion is a key parameter and is limited by the polymer permeability, chemical reactivity and geometry. We have seen by micro-FTIR that during the irradiation of the NBR/PVC film, a marked oxidation profile appeared. The predominant reaction is the crosslinking process, which results from the strongly oxidized and crosslinked layer in the first microns at the surface leading to a fragile layer versus the bulk of the sample which remains ductile and undegraded: when a stress is applied to the elastomeric material, cracks appear and propagate. For the thermooxidized sample, for 2 mm thick specimens or thin films, the oxidation seems to be homogeneous, and a general embrittlement is observed.

3.4. Correlation

In the first part of this study, we have shown that the degradation of the NBR/PVC blend during photo- and thermooxidation comes from a chain radical oxidation mechanism that leads to:

- Formation of crosslinking bridges through macroradical recombination,
- Changes in the three-dimensional network (demonstrated by DMTA analysis and tan δ evolution),
- Increase in the hardness value coming from the crosslinking reaction.

In the second part, we aimed to demonstrate that correlations exist between the changes observed at the different scales [48,50–52]**.** The parameters chosen to follow the degradation were the decrease in absorbance of the IR band at 966 cm^{-1}, the relative conversion ∝ versus time of the Shore A hardness, the swelling and the T_g measurements. The Eq.12 was used to calculate ∝

$$\propto = \frac{C_0 - C_t}{C_0} \qquad \textit{Eq.12}$$

where C_0 is the criteria value at t=0 and C_t is the criteria value at instant t.

3.4.1. Photo-ageing

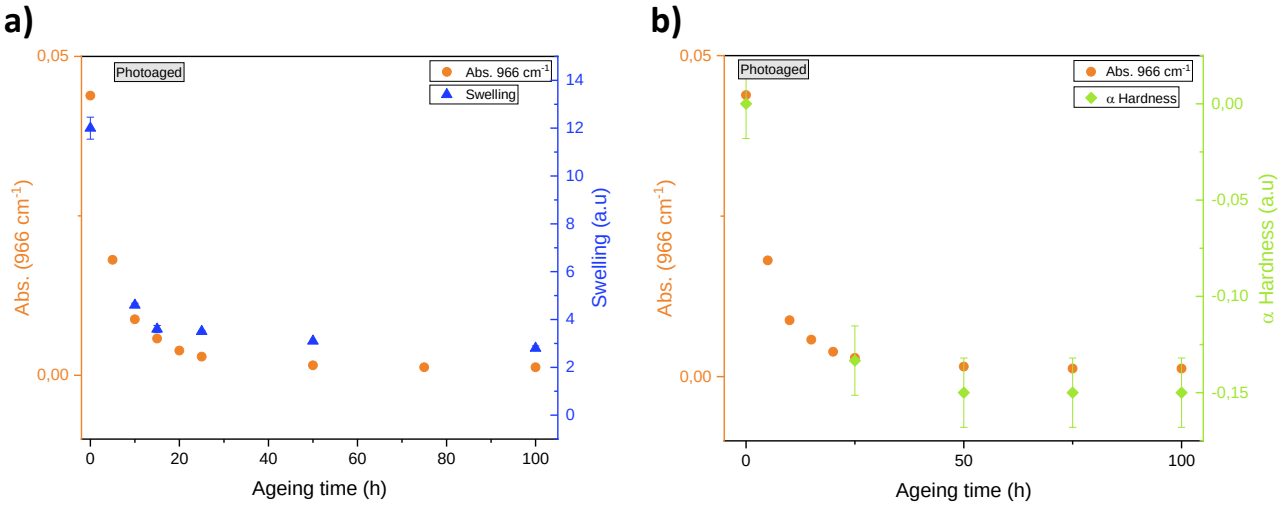

Figure 17. (a): Absorbance at 966 cm^{-1} (●) and swelling (▲) versus photooxidation time, (b): Absorbance at 966 cm^{-1} (●) and shore A hardness conversion rate (♦) versus photooxidation time

In the case of the photooxidized NBR/PVC blend, the decrease in absorbance at 966 cm^{-1} measured by infrared spectroscopy would be related to the formation of a denser three-dimensional network. This network would then be responsible for the decrease in the swelling rate and the increase in the surface hardness. To check if there were correlations between these parameters, we superimposed the evolution of the absorbance at 966 cm^{-1} monitored by ATR-Ge (a surface analysis) and the swelling rate evolution (Figure 17a) or the conversion rate of the shore hardness A evolution (Figure 17b) as a function of the photooxidation time. All these techniques correspond to surface analysis and allow us to only characterize the degraded layer of the polymer due to the oxidation profile plotted in Figure 11, showing that only a few microns are impacted by UV light under irradiation. Figure 17 shows that the curves follow the same trend, that is, an exponential decline, which confirms the relationships linking these phenomena together. The disappearance of the unsaturation

bands detected at 966 cm^{-1} would be at the origin of the visible modifications at the macromolecular scale and the losses of functional properties with a more important stiffness after photooxidation. This result is in good agreement with the previous work of C. Adam *et al*. [7,13], which associated the consumption of this IR band with the formation of crosslinking bridges during ageing.

3.4.2. Thermal ageing

a) **b)**

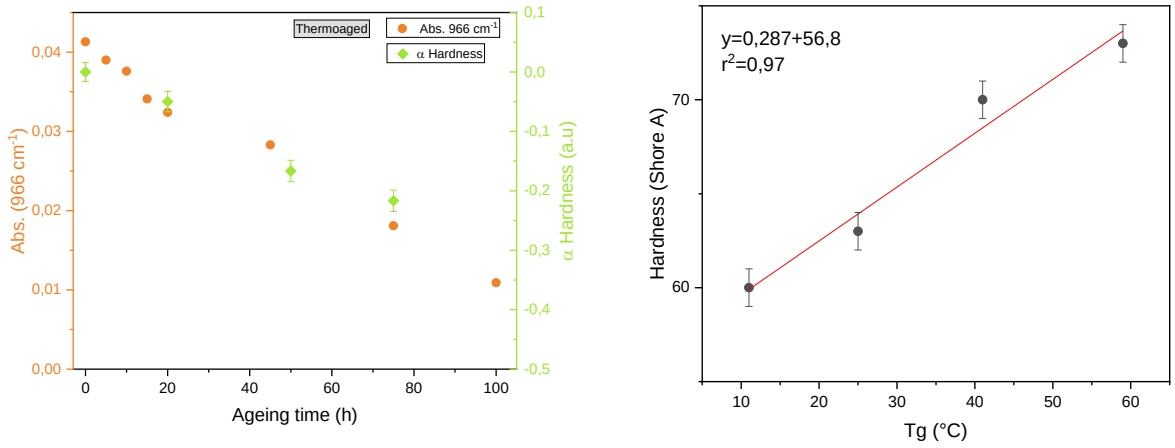

Figure 18. (a): Absorbance at 966 cm^{-1} (●) and shore A hardness (♦) conversion rate versus thermoooxidation time, (b): Shore A hardness values versus T_g

For the thermooxidized NBR/PVC blend, the superimposed absorbance at 966 cm^{-1} and the conversion rate of the shore hardness A evolution as a function of thermoooxidation time are presented in Figure 18 We observe that both curves follow a linear decrease. We can therefore conclude that these parameters are correlated. Moreover, the shore hardness A as a function of the glass transition temperature T_g was plotted in Figure 18b based on previous work relating these two parameters [52]. We observe a linear correlation, allowing us to conclude that the increase in glass transition temperature T_g during thermoooxidation is linked to the increase in hardness of the material.

We have then highlighted the relationships that exist between changes in the chemical structure of the material (consumption of double bonds), which lead to changes in the macromolecular architecture (loss of mobility, reduction of the network meshes), and the loss of use properties (stiffness).

Conclusion

The aim of this work was to understand the formation or not of cracks for cured NBR/PVC blends under photooxidation and thermoooxidation conditions. In both cases, the radical chain oxidation mechanism of the polymer leads to the formation of oxidation products, such as carboxylic acids, and a decrease of unsaturations identified by infrared spectroscopy, but also to crosslinking reactions. The oxidation products and kinetic curves showed that NBR is the main contributor to NBR/PVC blend degradation because of its butadiene sequences,

which are the weak points. Furthermore, a strong oxidation profile within photooxidized samples leads to different properties between the extreme surface, which is oxidized and crosslinked, and the bulk of the NBR/PVC film, where no chemical modifications occur. This heterogeneous degradation between the surface and the bulk can explain the occurrence of cracks on the surface of the material, which means a loss of functional properties. After thermoooxidation, the oxidation is more homogeneous, and the sample becomes brittle but does not present cracks.

In the second part, we showed that there is a good correlation between modifications of the chemical structure and those observed at other scales of analysis to prove that cracks are induced by UV–light irradiation in the presence of oxygen. The formation of oxidation products was connected to the decrease in the swelling ratio and the decrease of M_c of the NBR/PVC blend, providing evidence for crosslinking reaction and densification of the network as the main cause of degradation.

References

(1) Agarwal, K.; Prasad, M.; Chakraborty, A.; Vishwakarma, C. B.; Sharma, R. B.; Setua, D. K. Studies on Phase Morphology and Thermo-Physical Properties of Nitrile Rubber Blends. *J Therm. Anal. Calorim* **2011**, *104* (3), 1125–1133. https://doi.org/10.1007/s10973-010-1193-y.

(2) Manoj, N. R.; De, P. P. An Investigation of the Chemical Interactions in Blends of Poly(Vinyl Chloride) and Nitrile Rubber during Processing. *Polymer* **1998**, *39* (3), 733–741. https://doi.org/10.1016/S0032-3861(97)00281-4.

(3) George, K. E.; Joseph, R.; Francis, D. J. Studies on NBR/PVC Blends. *J. Appl. Polym. Sci.* **1986**, *32* (1), 2867–2873. https://doi.org/10.1002/app.1986.070320102.

(4) Wang, C. B.; Cooper, S. L. Morphology and Properties of Poly(Vinyl Chloride)–Poly(Butadiene-Co-Acrylonitrile) Blends. *J. Polym. Sci. Polym. Phys. Ed.* **1983**, *21* (1), 11–27. https://doi.org/10.1002/pol.1983.180210102.

(5) Sathaye, A.; Parkhi, S. Y.; Haridas, J. D. Experimental Optimization of NBR/PVC Formulation for Automobile Rubber Components; 2008; pp 2008-01–1472. https://doi.org/10.4271/2008-01-1472.

(6) Skowronski, T. A.; Rabek, J. F.; Rånby, B. Photo-Oxidation of Copolymers of Butadiene and Acrylonitrile. *Polym. Degrad. Stab.***1983**, *5* (3), 173–188. https://doi.org/10.1016/0141-3910(83)90008-3.

(7) Adam, C.; Lacoste, J.; Lemaire, J. Photo-Oxidation of Elastomeric Materials: Part 3 - Photo-Oxidation of Acrylonitrile-Butadiene Copolymer. *Polym. Degrad. Stab.* **1990**, *27* (1), 85–97. https://doi.org/10.1016/0141-3910(90)90099-S.

(8) Scott, G.; Tahan, M. Comparison of the Photo-Oxidative Behaviour of Some Polybutadiene-Based Polyblends. *Eur. Polym. J.* **1977**, *13* (12), 981–987. https://doi.org/10.1016/0014-3057(77)90170-7.

(9) Delor-Jestin, F.; Barrois-Oudin, N.; Cardinet, C.; Lacoste, J.; Lemaire, J. Thermal Ageing of Acrylonitrile-Butadiene Copolymer. *Polym. Degrad. Stab***. 2000**, *70* (1), 1–4. https://doi.org/10.1016/S0141-3910(00)00035-5.

(10) Grassie, N.; Heaney, A. Thermal Degradation of Copolymers of Butadiene and Acrylonitrile. *Eur. Polym.* **1974**, *10*, 415–424.

(11) Liu, J.; Li, X.; Xu, L.; Zhang, P. Investigation of Aging Behavior and Mechanism of Nitrile-Butadiene Rubber (NBR) in the Accelerated Thermal Aging Environment. *Polym. Test.* **2016**, *54*, 59–66. https://doi.org/10.1016/j.polymertesting.2016.06.010.

(12) Pazur, R. J.; Cormier, J. G.; Korhan-Taymaz, K. The Effect Of Acrylonitrile Content On The Thermo-Oxidative Aging Of Nitrile Rubber. *Rub. Chem. Technol.* **2014**, *87* (1), 53–69. https://doi.org/10.5254/rct.13.87937.

(13) Adam, C.; Lacoste, J.; Lemaire, J.; Pascal, B. Photo-Oxidation of Elastomeric Materials. Part I-Photo- Oxidation of Polybutadienes. *Polym. Degrad. Stab.* **1989**, *24*, 185–200.

(14) Kagiya, V. T.; Takemoto, K. Crosslinking and Oxidation of 1, 2-Polybutadiene by UV Irradiation. *J. Macromol. Sci.: Part A - Chemistry* **1976**, *10* (5), 795–810. https://doi.org/10.1080/00222337608061218.

(15) Piton, M.; Rivaton, A. Photooxidation of Polybutadiene at Long Wavelengths (Λ>300nm). *Polym. Degrad. Stab.* **1996**, *53*, 343–359.

(16) Gardette, J. L.; Gaumet, S.; Lemaire, J. Photooxidation of Poly(Vinyl Chloride). 1. A Reexamination of the Mechanism. *Macromol.***1989**, *22* (6), 2576–2581. https://doi.org/10.1021/ma00196a005.

(17) Gardette, J.-L.; Lemaire, J. Wavelength Effects on the Discoloration and Oxidation of Poly(Vinyl Chloride). *Polym. Degrad. Stab.* **1989**, *25* (2–4), 293–306. https://doi.org/10.1016/S0141-3910(89)81013-4.

(18) Gardette, J.-L.; Lemaire, J. Photothermal and Thermal Oxidations of Rigid, Plasticized and Pigmented Poly(Vinyl Chloride). *Polym. Degrad. Stab.* **1991**, *34* (1–3), 135–167. https://doi.org/10.1016/0141-3910(91)90117-A.

(19) Hjertberg, T.; Sörvik, E. M. Thermal Degradation of PVC. In *Degradation and stabilisation of PVC*; **1984**; pp 21–80.

(20) Chen, X.; Wang, J.; Shen, J. Effect of UV-Irradiation on Poly(Vinyl Chloride) Modified by Methyl Methacrylate–Butadiene–Styrene Copolymer. *Polym. Degrad. Stab.* **2005**, *87* (3), 527–533. https://doi.org/10.1016/j.polymdegradstab.2004.10.010.

(21) Kawashima, T.; Ogawa, T. Prediction of the Lifetime of Nitrile-Butadiene Rubber by FT-IR. *Anal. Sci.* **2005**, *21* (12), 1475–1478. https://doi.org/10.2116/analsci.21.1475.

(22) Kolawole, E. G.; Agboola, M. O. Environmental Degradation of Some Polymer Blends. Blends of Polystyrene with Acrylonitrile Butadiene Styrene, Poly(Vinyl Chloride), and Polybutadiene and Blends of Polybutadiene with Poly(Vinyl Chloride). *J. Appl. Polym. Sci.* **1982**, *27* (7), 2317–2335. https://doi.org/10.1002/app.1982.070270702.

(23) Chai, R. D.; Zhang, J. Synergistic Effect of Hindered Amine Light Stabilizers/Ultraviolet Absorbers on the Polyvinyl Chloride/Powder Nitrile Rubber Blends during Photodegradation. *Polym. Eng. Sci.* **2013**, *53* (8), 1760–1769. https://doi.org/10.1002/pen.23432.

(24) Mailhot, B.; Morlat, S.; Gardette, J.-L. Photooxidation of Blends of Polystyrene and Poly(Vinyl Methyl Ether): FTIR and AFM Studies. *Polymer* **2000**, *41* (6), 1981–1988. https://doi.org/10.1016/S0032-3861(99)00204-9.

(25) Lala, D.; Rabek, J. F.; Rånby, B. Photo-Degradation and Photo-Stabilisation of the Two-Phase System Poly(Vinyl Chloride)-Polybutadiene. *Polym. Degrad. Stab.* **1981**, *3* (4), 307–321. https://doi.org/10.1016/0141-3910(81)90026-4.

(26) Waldman, W. R.; De Paoli, M.-A. Photodegradation of Polypropylene/Polystyrene Blends: Styrene–Butadiene–Styrene Compatibilisation Effect. *Polym. Degrad. Stab***. 2008**, *93* (1), 273–280. https://doi.org/10.1016/j.polymdegradstab.2007.09.003.

(27) Skowronski, T.; Rabek, J. F.; Rånby, B. Photodegradation of Some Poly(Vinyl Chloride) (PVC) Blends: PVC/Ethylene-Vinyl Acetate (EVA) Copolymers and PVC/Butadiene-Acrylonitrile (NBR) Copolymers: Photodegradation of Some Poly(Vinyl Chloride) (PVC) Blends. *Polym. Eng. Sci.* **1984**, *24* (4), 278–286. https://doi.org/10.1002/pen.760240409.

(28) Flory, P. J.; Rehner, J. Statistical Mechanics of Cross-Linked Polymer Networks II. Swelling. *The J. Chem. Phys.***1943**, *11* (11), 521–526. https://doi.org/10.1063/1.1723792.

(29) Kraus, G. Swelling of Filler-Reinforced Vulcanizates. *J. Appl. Polym. Sci.* **1963**, *7* (3), 861–871. https://doi.org/10.1002/app.1963.070070306.

(30) Guth, E. Theory of Filler Reinforcement. *J. Appl. Phys.* **1945**, *16* (1), 20–25.

(31) Sosson, F. Evolution Des Propriétés Viscoélastiques d'élastomères Chargés Soumis à Des Sollicitations Mécaniques Dynamiques, Université du sud Toulon-Var, **2007**.

(32) Baba, M.; Gardette, J.-L.; Lacoste, J. Crosslinking on Ageing of Elastomers: I. Photoageing of EPDM Monitored by Gel, Swelling and DSC Measurements. *Polym. Degrad. Stab.* **1999**, *63* (1), 121–126. https://doi.org/10.1016/S0141-3910(98)00080-9.

(33) Mertz, G. Evolution Des Propriétés Physico-Chimiques et Mécaniques de Composite à Base de Caoutchoucs Lors Du Photo-Vieillissement, Institut National Polytechnique de Lorraine, **2011**.

(34) Delor-Jestin, F. Comportement Thermique et Photochimique à Long Terme d'élastomères Pour Applications Dans Le Secteur Automobile, Université Blaise Pascal, **1996**.

(35) Xiaojiang, Z.; Pu, H. H.; Yanheng, Y.; Junfeng, L. A FT-IR Study on NBR / PVC, BR / PVC, and BR / PVC / NBR Blends. *J. Polym. Sci. C Polym. Lett.* **1989**, *27* (7), 223–227. https://doi.org/10.1002/pol.1989.140270702.

(36) Krimm, S.; Folt, V. L.; Shipman, J. J.; Berens, A. R. Infrared Spectra and Assignments for Polyvinyl Chloride and Deuterated Analogs. *J. Polym. Sci. A Gen. Pap.* **1963**, *1* (8), 2621–2650. https://doi.org/10.1002/pol.1963.100010809.

(37) Rabek, Jan. F. *Polymer Photodegradation*; Springer Netherlands: Dordrecht, **1995.** https://doi.org/10.1007/978-94-011-1274-1.

(38) Rånby, B. Photodegradation and Photo-Oxidation of Synthetic Polymers. *J. Anal. Appl. Pyr.* **1989**, *15*, 237–247. https://doi.org/10.1016/0165-2370(89)85037-5.

(39) Scott, G. Initiation Processes in Polymer Degradation. *Polym. Degrad. Stab***. 1995**, *48* (3), 315–324. https://doi.org/10.1016/0141-3910(95)00090-9.

(40) Mailhot, B.; Bussière, P.-O.; Rivaton, A.; Morlat-Therias, S.; Gardette, J.-L. Depth Profiling by AFM Nanoindentations and Micro-FTIR Spectroscopy for the Study of Polymer Ageing. *Macromol. Rapid Commun.* **2004**, *25* (2), 436–440. https://doi.org/10.1002/marc.200300110.

(41) Celina, M.; Wise, J.; Ottesen, D. K.; Gillen, K. T.; Clough, R. L. Oxidation Profiles of Thermally Aged Nitrile Rubber. *Polym. Degrad. Stab.* **1998**, *60* (2–3), 493–504. https://doi.org/10.1016/S0141-3910(97)00113-4.

(42) Zhao, J.; Yang, R.; Iervolino, R.; Barbera, S. Changes Of Chemical Structure And Mechanical Property Levels During Thermo-Oxidative Aging Of Nbr. *Rub. Chem. Technol.* **2013**, *86* (4), 591–603. https://doi.org/10.5254/RCT.13.87969.

(43) Budrugeac, P. Thermooxidative Degradation of Some Nitrile-Butadiene Rubbers. *Polym. Degrad. Stab.* **1992**, *38* (2), 165–172. https://doi.org/10.1016/0141-3910(92)90010-3.

(44) Halary, J. L.; Laupetre, F.; Monnerie, L. *Mécanique de Matériaux Polymères*, Belin.; **2008**.

(45) Musto, P.; Ragosta, G.; Abbate, M.; Scarinzi, G. Photo-Oxidation of High Performance Epoxy Networks: Correlation between the Molecular Mechanisms of Degradation and the Viscoelastic and Mechanical Response. *Macromol.* **2008**, *41* (15), 5729–5743. https://doi.org/10.1021/ma8005334.

(46) Manoj, N. R.; De, P. P.; De, S. K. Self-Crosslinkable Plastic-Rubber Blend System Based on Poly (Vinyl Chloride) and Acrylonitrile-Co-Butadiene Rubber. *J. Appl. Polym. Sci.* **1993**, *49* (1), 133–142. https://doi.org/10.1002/app.1993.070490116.

(47) Manoj, N. R.; De, P. P. Hot Air and Fuel Ageing of Poly(Vinyl Chloride)/Nitrile Rubber and Poly(Vinyl Chloride) /Hydrogenated Nitrile Rubber Blends. *Polym. Degrad. Stab.* **1994**, *44* (1), 43-47. https://doi.org/10.1016/0141-3910(94)90030-2.

(48) Berthumeyrie, S.; Collin, S.; Bussiere, P.-O.; Therias, S. Photooxidation of Cellulose Nitrate: New Insights into Degradation Mechanisms. *J. Hazard. Mater.* **2014**, *272*, 137–147. https://doi.org/10.1016/j.jhazmat.2014.02.039.

(49) Halary, J. L.; Lauprêtre, F. *De La Macromolécule Au Matériau Polymère*, Belin.; **2006**.

(50) Peng, Y.-Y.; Diaz Dussan, D.; Narain, R. Thermal, Mechanical, and Electrical Properties. In *Polymer Science and nanotechnology: fundamentals and applications*; Elsevier Applied Science, **2020**; pp 179–201.

(51) Larché, J.-F.; Bussière, P.-O.; Therias, S.; Gardette, J.-L. Photooxidation of Polymers: Relating Material Properties to Chemical Changes. *Polym. Degrad. Stab.* **2012**, *97* (1), 25–34. https://doi.org/10.1016/j.polymdegradstab.2011.10.020.

(52) Fakirov, S.; Balta Calleja, F. J.; Krumova, M. On the Relationship between Microhardness and Glass Transition Temperature of Some Amorphous Polymers. *J. Polym. Sci.* **1999**, *37*, 1413–1419.